Hindawi
Complexity
Volume 2020, Article ID 8844657, 11 pages
https://doi.org/10.1155/2020/8844657

WILEY | Hindawi

Research Article

Multistability in a Fractional-Order Centrifugal Flywheel Governor System and Its Adaptive Control

Bo Yan,[1] **Shaobo He**,[2] **and Shaojie Wang**[1]

[1]*College of Electrical and Information Engineering, Shaoyang University, Shaoyang 422000, China*
[2]*School of Physics and Electronics, Central South University, Changsha 410083, China*

Correspondence should be addressed to Shaobo He; heshaobo_123@163.com

Received 1 October 2020; Revised 16 November 2020; Accepted 24 November 2020; Published 14 December 2020

Academic Editor: Zhouchao Wei

In this paper, a 4D fractional-order centrifugal flywheel governor system is proposed. Dynamics including the multistability of the system with the variation of system parameters and the derivative order are investigated by Lyapunov exponents (LEs), bifurcation diagram, phase portrait, entropy measure, and basins of attraction, numerically. It shows that the minimum order for chaos of the fractional-order centrifugal flywheel governor system is $q = 0.97$, and the system has rich dynamics and produces multiple coexisting attractors. Moreover, the system is controlled by introducing the adaptive controller which is proved by the Lyapunov stability theory. Numerical analysis results verify the effectiveness of the proposed method.

1. Introduction

The centrifugal flywheel governor system is a device for automatically adjusting and controlling the speed of the engine. It has opened the precedent of modern automatic control, marked the birth of modern automatic control technology, and been widely used in modern industry. When the centrifugal flywheel governor system is disturbed, the velocity of the system will change suddenly and the chaotic vibration will be produced [1, 2]. In order to make the centrifugal governor system run stably and play a good role in practical application, it is necessary to study the chaotic dynamics law when the system is disturbed and how to control the chaotic motion to the stable state.

In recent years, the research on chaos and control of the centrifugal flywheel governor system has attracted wide attention of scholars [3–14]. For example, Zhang et al. [3] studied the evolution from Hopf bifurcation to chaos of the centrifugal flywheel governor system subjected to external distance. Gou et al. [4–9] analyzed the chaos forming process of the centrifugal flywheel governor system by the bifurcation diagram, the phase portrait, and Poincare map and controlled the chaotic behavior to the steady orbit by linear and nonlinear feedback control methods. Zhang et al. [10] studied complex dynamical behavior of a class of the centrifugal flywheel governor system and proposed a parametric open-plus-closed-loop approach to control chaos motion to any desired periodic orbit. Rao et al. [11] investigated the global structure of nonlinear response of mechanical centrifugal governor and found a new type of mixed-mode oscillations in the periodic response. Luo et al. [12] addressed chaos suppression of the mechanical centrifugal flywheel governor system with output constraint and fully unknown parameters via adaptive dynamic surface control. Aghababa et al. [13] derived an adaptive robust controller to suppress the chaos of nonautonomous centrifugal flywheel governor systems in a given finite time effectively by using the adaptation laws and Lyapunov control theory. Zhang et al. [14] studied the Hopf bifurcation of the typical autonomous and nonautonomous centrifugal flywheel governor system and discussed the reason of chaotic oscillation of the system.

As far as we know, the fractional-order derivative has been proposed for more than 300 years. It becomes to be a research hotspot in the nonlinear research field. Unlike the integer-order differential operator, the fractional-order differential operator can effectively describe the

physical process with historical memory effect, for instance, Caputo definition and Riemann–Liouville definition [15]. Those fractional calculus have been widely used in theoretical analysis and engineering. Specifically, they have been used in different research fields such as quantum mechanics, electromagnetic oscillation, system control, material mechanics, and other fields [16–19]. Therefore, it is of great theoretical significance to introduce fractional calculus into the study on chaos and control of the centrifugal flywheel governor system. For example, Ge et al. [20] determined the existence of chaos in the fractional-order autonomous and nonautonomous nonlinear centrifugal flywheel governor system by using the bifurcation diagram and phase portrait and realized chaos control of the system by the linear feedback control method. But, the research on chaos and control of the fractional-order system needs to be further expanded, and this study provides a useful reference for the further research of the fractional-order centrifugal flywheel governor system.

In this paper, chaos and its adaptive control of the fractional-order centrifugal flywheel governor system are studied. The outline of this paper is given as follows. In Section 2, the fractional-order centrifugal flywheel governor system is introduced. In Section 3, dynamics of the integer-order centrifugal flywheel governor system are investigated numerically by the bifurcation diagram, LEs, the phase portrait, and the basins of attraction. In Section 4, the adaptive control formula is derived and the chaos control of the system is realized by simulation. In Section 5, the results are summarized.

2. The Fractional-Order Centrifugal Flywheel Governor System

The mechanics model of the centrifugal flywheel governor with external disturbance is depicted in Figure 1, where l, m, r, and ϕ represent the length of the rod, the mass of the fly ball, the distance between the rotational axis and the suspension joint, and the angle between the rotational axis and the rod, respectively. The motor drives the flywheel to rotate with angular velocity ω. The flywheel is joined to the axis through a gear box, so the axis rotates with angular velocity $n\omega$. n is the proportional coefficient, k is the stubborn coefficient of the spring, and g is the gravitational acceleration. Ignoring the mass of the pipe and casing and assuming that the damping coefficient at the joint of the rod head and the ball is c, the motion equation of the system is given by [10, 14]

$$2\left[ml^2\ddot{\phi} - mrl\eta^2\cos\phi - \left(2k + m\eta^2\right)l^2\sin\phi\cos\phi + (2kl + mg)l\sin\phi\right] = -c\dot{\phi}. \tag{1}$$

For the rotational machine, the net torque is the difference between the torque Q produced by the engine and the load torque Q_L, which is available for angular acceleration, which is

$$J\frac{\mathrm{d}\omega}{\mathrm{d}t} = Q - Q_L, \tag{2}$$

where J is the moment of inertia of the machine. As the angle ϕ varies, the position of the control valve which admits the fuel is also varied. Then, equation (2) can be written in the form:

$$J\dot{\omega} = \gamma\cos\phi - \beta, \tag{3}$$

where $\gamma > 0$ is a proportionally constant and β is an equivalent torque of the load. Let

$$\begin{aligned} s &= \frac{\gamma}{J\Omega_n}, \\ F &= \frac{\beta}{J\Omega_n}, \\ d &= \frac{n^2 m}{2\mathrm{kl} + \mathrm{mg}}, \\ b &= \frac{c}{2\mathrm{ml}^2\Omega_n}, \\ e &= \frac{2\mathrm{kl}}{2\mathrm{kl} + \mathrm{mg}}, \\ p &= \frac{n^2\mathrm{ml}}{2\mathrm{kl} + \mathrm{mg}}, \\ \Omega_n &= \sqrt{\frac{2\mathrm{kl} + \mathrm{mg}}{\mathrm{ml}}}, \end{aligned} \tag{4}$$

and change time scale $\tau = \Omega_n t$; let $\varphi = \mathrm{d}\phi/\mathrm{d}\tau$, $x = \phi$, $y = \varphi$, and $z = \omega$, then equation (1) can be written as the standard form of the three-dimensional autonomy system:

$$\begin{cases} \dot{x} = y, \\ \dot{y} = dz^2\cos x + \left(e + pz^2\right)\sin x\cos x - \sin x - by, \\ \dot{z} = s\cos x - F. \end{cases} \tag{5}$$

The above system (4) is proposed with the assumption that the load torque is constant. When the load torque is not constant, it can be represented by a constant term F and a Hamiltonian term $\alpha\sin(\sigma t)$, where F, α, and σ are constants. Then, (4) can be written as

$$\begin{cases} \dot{x} = y, \\ \dot{y} = dz^2\cos x + \left(e + pz^2\right)\sin x\cos x - \sin x - by, \\ \dot{z} = s\cos x - F - \alpha\sin(\sigma t). \end{cases} \tag{6}$$

Let $\sigma t = w$, we can get $\dot{w} = \sigma$ and then equation (6) becomes

$$\begin{cases} \dot{x} = y, \\ \dot{y} = dz^2\cos x + \left(e + pz^2\right)\sin x\cos x - \sin x - by, \\ \dot{z} = s\cos x - F - \alpha\sin(w), \\ \dot{w} = \sigma. \end{cases} \tag{7}$$

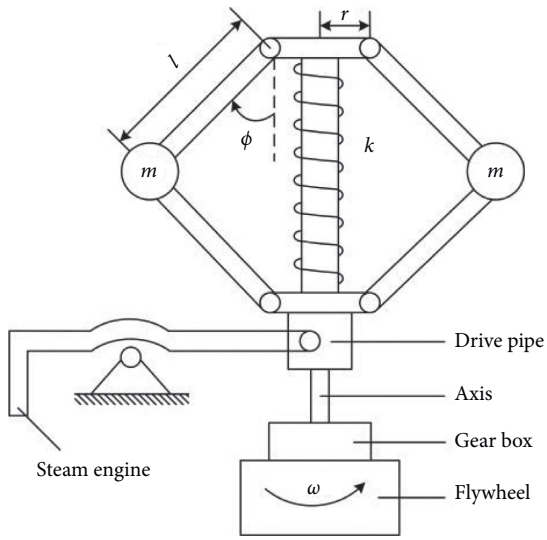

Figure 1: The mechanics model of the centrifugal flywheel governor system.

By introducing the fractional-order derivative to system (7), the fractional-order centrifugal flywheel governor system is obtained, and it is defined by

$$\begin{cases} D_{t_0}^q x = y, \\ D_{t_0}^q y = dz^2 \cos x + \left(e + pz^2\right)\sin x \cos x - \sin x - by, \\ D_{t_0}^q z = s\cos x - F - \alpha \sin(w), \\ D_{t_0}^q w = \sigma, \end{cases} \tag{8}$$

where $D_{t_0}^q$ is the q-order Caputo differential operator [21, 22]. The Caputo fractional-order derivative definition is given by

$$D_{t_0}^q x(t) = \begin{cases} \dfrac{1}{\Gamma(1-q)} \displaystyle\int_{t_0}^{t} \frac{\dot{x}(\tau)}{(t-\tau)} d\tau, & 0 < q < 1, \\ \dot{x}(t), & q = 1, \end{cases} \tag{9}$$

where $q \in R^+$ and $\Gamma(\cdot)$ is the Gamma function.

3. Multistability Analysis

In this section, the bifurcation diagram, LEs, phase portrait, and the basins of attraction are employed to investigate the dynamics of the fractional-order centrifugal flywheel governor system. In the following analyses, we fix the system parameters $d = 0.08$, $p = 0.01$, $e = 0.5$, $b = 0.4$, $F = 1.942$, $\alpha = 0.4$, and $\sigma = 1.0$ and select parameter s as the argument variable. The system is numerically solved by the predictor-corrector algorithm [23–25]. The Matlab source code named "FDE12.m" of the predictor-corrector method can be downloaded online [26]. The method of using "FDE12.m" to solve the fractional-order system is described in detail in reference [27]. The detailed numerical solutions and how to compute LEs of the fractional-order system can be obtained according to reference [28]. The predictor-corrector algorithm is an effective method to solve the fractional-order partial differential equation. For example, Oskouie et al. [24] used the predictor-corrector algorithm to solve the fractional viscoelastic Bernoulli nanobeams differential equation and investigated the effects of fractional derivative order, surface parameters, and others factors on the nonlinear time response. He et al. [25] investigated a fractional-order microscopic chemical system by the predictor-corrector algorithm.

3.1. Bifurcation Analysis. Dynamics of the system with the variation of g and q are analyzed by means of bifurcation diagram, LEs, and phase diagrams. Four cases are investigated.

3.1.1. Case 1. Fix $s = 10$ and vary the derivative order q from 0.94 to 1 with the step size of 3×10^{-4}. Set the initial condition as $[x_0, y_0, z_0, w_0] = [0.005, 0.005, -0.1, 0.1]$ and $[0.5, 0.005, -0.1, 0.1]$. The bifurcation diagram and LEs of the fractional-order centrifugal flywheel governor system are illustrated in Figure 2. In Figure 2(a), blue points represent $x_{\max}$ for the initial values $[x_0, y_0, z_0, w_0] = [0.005, 0.005, -0.1, 0.1]$ and red points for $[x_0, y_0, z_0, w_0] = [0.5, 0.005, -0.1, 0.1]$. But. Figure 2(b) only shows LEs for $[x_0, y_0, z_0, w_0] = [0.005, 0.005, -0.1, 0.1]$. It can be seen from Figure 2 that the system is chaotic when $q > 0.963$, and for other values of q, the system is convergent. Through LE curves in Figure 2(b), we can see that when $q \in [0.963, 0.97]$, the system is not chaotic. But, when $q > 0.97$, the system always has a positive Lyapunov exponent, which shows the system is always in a chaotic state. In addition, the complexity of the system increases with the increase in derivative order q. Therefore, for the fractional-order centrifugal flywheel governor system, the LE curve is more accurate in describing the state of the system than the bifurcation diagram. It can well describe the process of transition from period to chaos. Figure 3(a) shows that when $[x_0, y_0, z_0, w_0] = [0.5, 0.005, -0.1, 0.1]$, the minimum order for chaos of the system is increased but the shape of the bifurcation diagram keeps unchanged which means the initial condition will affect the dynamics of the system. The periodic circles for $q = 0.94$ and 0.968 and chaotic attractors for $q = 0.972$ and 0.99 are shown in Figure 4. It can be seen that the result of phase portrait analysis is consistent with the result of dynamic characteristic analysis, and the chaotic attractors show obvious chaotic characteristic.

3.1.2. Case 2. Fix $q = 0.98$; let the parameter s vary from 2 to 18 with the step size of 0.08, and the initial condition also be $[x_0, y_0, z_0, w_0] = [0.005, 0.005, -0.1, 0.1]$ and $[0.5, 0.005, -0.1, 0.1]$, and then dynamical analysis results are shown in Figure 4. In Figure 4(a), blue points represent $x_{\max}$ for the initial values $[x_0, y_0, z_0, w_0] = [0.005, 0.005, -0.1, 0.1]$ and red points for the initial values $[x_0, y_0, z_0, w_0] = [0.5, 0.005, -0.1, 0.1]$. But, Figure 4(b) only shows LEs for $[x_0, y_0, z_0, w_0] =$

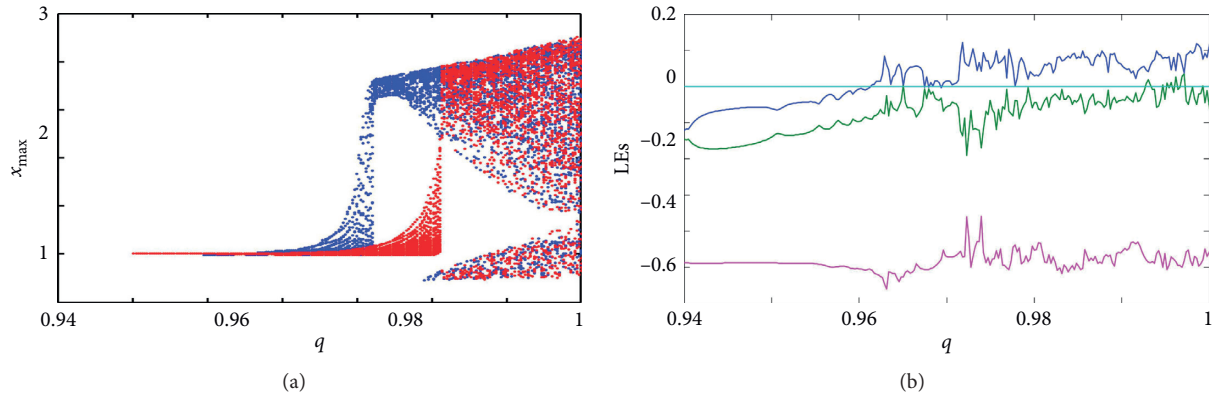

FIGURE 2: The dynamics of the fractional-order centrifugal flywheel governor system vary with derivative order q. (a) Bifurcation diagram. (b) Lyapunov exponent spectrum.

[0.005, 0.005, −0.1, 0.1]. It shows in Figure 4 that the system is chaotic for $s \in [3.5, 13.5]$ and [2.9, 3.1] and is convergent for other values of s. In addition, when $s \in [6, 10]$, the complexity of the system is relatively large. Figure 4(a) shows that when $[x_0, y_0, z_0, w_0] = [0.5, 0.005, -0.1, 0.1]$, the larger complexity interval is reduced, which means that the system will produce the coexistence attractors with different initial conditions.

3.1.3. Case 3. Let the parameter $s \in [3, 15]$ and derivative order $q \in [0.96, 1]$; divide the parameter space into a 150×150 grid. As with above cases, the initial condition is given by $[x_0, y_0, z_0, w_0] = [0.005, 0.005, -0.1, 0.1]$. Then, the maximum Lyapunov exponent-based contour plot in the parameter plane s-q is shown in Figure 5. It can be seen that the chaotic region is mainly observed in the area located in s $\in$ [4.8, 10] and $q \in [0.98, 1]$. In this area, the system has relative larger maximum Lyapunov exponents with lager q. In addition, when s $\in$ [5, 7.8] and $q \in [0.995, 1]$, the value of maximum Lyapunov exponents is bigger. Finally, it also can be found out that the minimum order for chaos is about $q = 0.927$.

3.1.4. Case 4. Fix $q = 0.98$ and $s = 10$, and the initial values are $[x_0, y_0, z_0, w_0] = [x_0, 0.005, -0.1, 0.1]$ and $x_0 \in [0, 2]$. The bifurcation diagram of the fractional-order centrifugal flywheel governor system is shown in Figure 6(a). Similarly, when $[x_0, y_0, z_0, w_0] = [0.005, y_0, -0.1, 0.1]$, $y_0 \in [0, 2]$. The bifurcation diagram of the system is plotted in Figure 6(b). It can be seen that when the initial condition changes, the complexity and state of the system are affected. In addition, different initial value components have different effects on the dynamics of the system. For Figure 6(a), the periodic state can be found at $x_0 = 1$. For Figure 6(b), the complexity is significantly different when $y_0 = 1.21$.

3.2. Basin of Attraction. The coexisting attractor is an important feature of chaotic systems, which has been studied by many scholars. For example, Lai et al. [29–31] used the dynamic evolution with respect to parameters and initial conditions to illustrate the existence coexisting attractors and presented the circuit implementation of the coexisting attractors for some chaotic systems. The basin of attraction is an effective tool to analyze multistability and the phenomenon of the coexistence of attractors [32].

In this paper, the method used is presented. For the proposed system, there are four state variables x, y, z, and w. Thus, four time series are obtained, and they can be defined as $\{x(n); y(n); z(n); w(n);\ n = 1, 2, 3, \ldots, N\}$, where N is the length of the time series. Then, the position of the attractor is defined by

$$P = [\overline{x}, \overline{y}, \overline{z}, \overline{w}], \tag{10}$$

where the mean values of each time series are used. The size of the attractor is given by

$$S = \left[S_x, S_y, S_z, S_w\right], \tag{11}$$

where $S_x = \max(x) - \min(x)$, $S_y = \max(y) - \min(y)$, $S_z = \max(z) - \min(z)$, and $S_w = \max(w) - \min(w)$. Suppose that there are two chaotic attractors, and their time series are defined by $\{x(n); y(n); z(n); w(n);\ n = 1, 2, 3, \ldots, N\}$ and $\{\widetilde{x}(n); \widetilde{y}(n); \widetilde{z}(n); \widetilde{w}(n);\ n = 1, 2, 3, \ldots, N\}$. The error between the positions of the two attractors is given by

$$e_1 = \frac{1}{4}\sqrt{(\overline{x} - \overline{\overline{x}})^2 + (\overline{y} - \overline{\overline{y}})^2} + (\overline{z} - \overline{\overline{z}})^2 + (\overline{w} - \overline{\overline{w}})^2 . \tag{12}$$

while the error regarding the size of the attractors is defined by

$$e_2 = \frac{1}{4}\sqrt{\left(S_x - \widetilde{S}_x\right)^2 + \left(S_y - \widetilde{S}_y\right)^2 + \left(S_z - \widetilde{S}_z\right)^2 + \left(S_w - \widetilde{S}_w\right)^2}. \tag{13}$$

In this paper, we set a parameter *error* to decide whether the obtained attractor is different with existing ones or not. Namely, if both $e_1 >$ error and $e_2 >$ error, the obtained attractor $\{\widetilde{x}(n); \widetilde{y}(n); \widetilde{z}(n); \widetilde{w}(n);\ n = 1, 2, 3, \ldots, N\}$ is a new attractor. Otherwise, it is not a new attractor. In this paper, the value of *error* is set as 50. The flow chart for basins of attraction is shown in Figure 7.

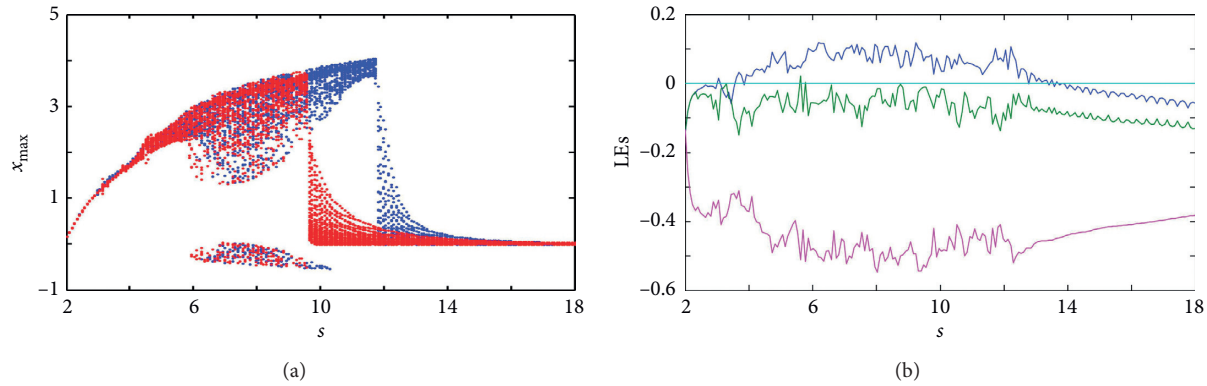

FIGURE 3: The dynamics of the fractional-order centrifugal flywheel governor system vary with parameter s; (a) Bifurcation diagram. (b) Lyapunov exponent spectrum.

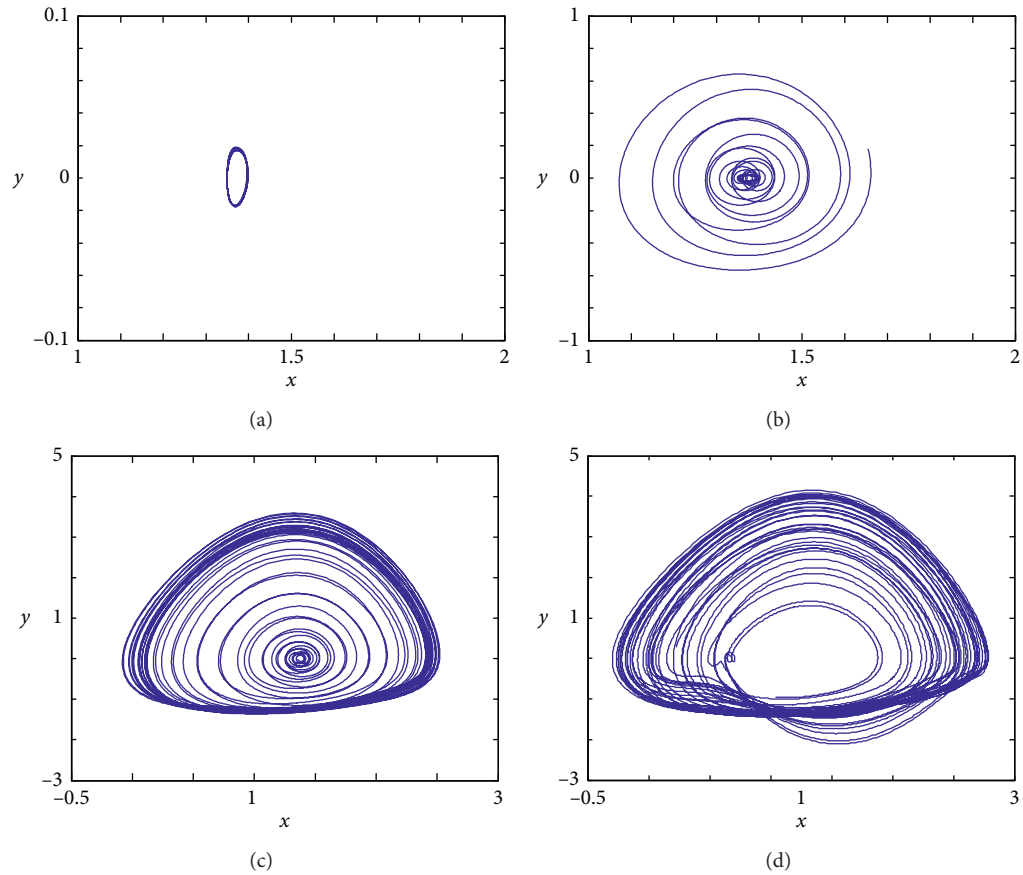

FIGURE 4: Phase diagrams with different derivative orders: (a) $q = 0.94$; (b) $q = 0.968$; (c) $q = 0.972$; (d) $q = 0.99$.

Fix $s = 10$ and the initial values are set as $[x_0, y_0, z_0, w_0] = [x, y, -0.1; 0.1]$. Variables x and y change from -1 to 1 with the step size of 0.01. Then, the basins of attraction in the x-y plane with different values of q are shown in Figures 8(a)–8(c). Similarly, fix $s = 5$, other conditions remain unchanged, and the responding basins of attraction in the x-y plane with different values of q are shown in Figures 8(d)–8(f). Different colours in Figure 8 represent different attraction fields, so we can see from Figure 8 that when the initial value of the system changes, the fractional-order centrifugal flywheel governor system shows coexisting attractors, and with the increase in derivative order q, the frequency of coexisting attractors increases gradually, but the range and shape of the different attractors remain basically unchanged.

Fix $q = 0.98$, $s = 10$, the initial conditions are given by $[x_0, y_0, z_0, w_0] = [0.005, 0.005, -0.1, 0.1]$, $[0.5, 0.005, -0.1, 0.1]$, and $[0.58, 0.005, -0.1, 0.1]$, and corresponding coexisting attractors are shown in Figures 9(a)–9(c). When $q = 0.99$ and

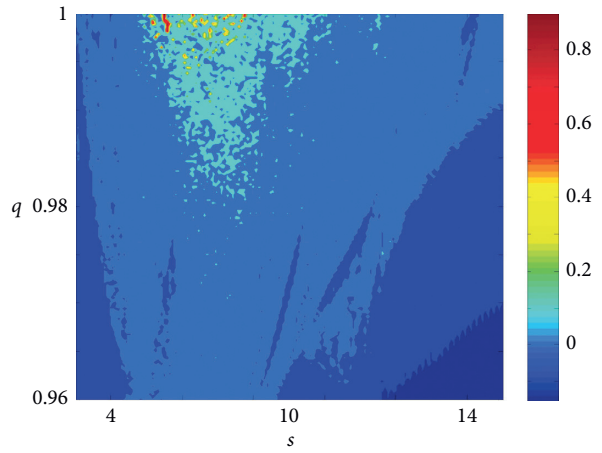

Figure 5: The chaos diagram of the maximum Lyapunov exponent contour plot in the s-q parameter plane.

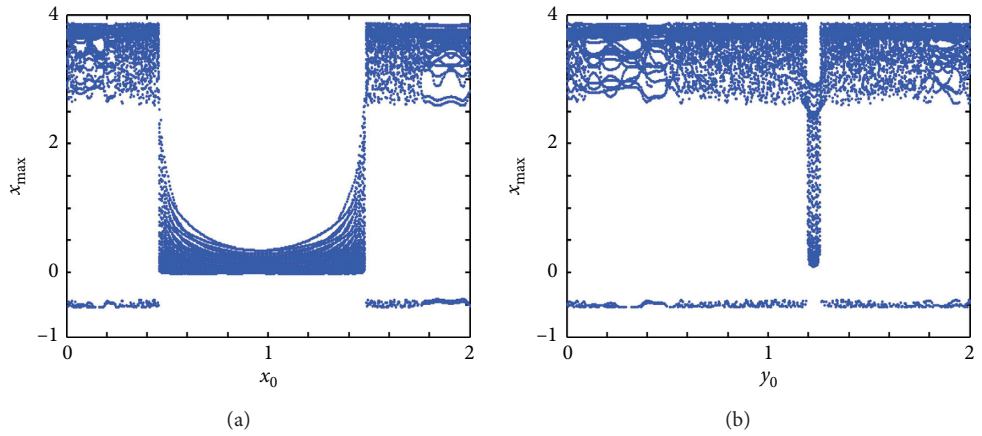

Figure 6: Bifurcation diagram of the fractional-order centrifugal flywheel governor system: (a) x_0 changes and (b) y_0 changes.

$s = 5$, coexisting attractors for the initial conditions $[x_0, y_0, z_0, w_0] = [-0.9, 0.1, -0.1, 0.1]$, $[-0.9, 0.82, -0.1, 0.1]$, and $[-0.9, 0.82, -0.1, 0.1]$ are shown in Figures 9(d)–9(f). Figure 9 shows that when the initial value of the system changes, the attractor of the system shows various states such as chaos, period, quasichaos. In addition, different kinds of chaotic attractors of the same state directly verify the simulation results as shown in (Figure 8).

4. Adaptive Control of Chaos

The process of controlling a chaotic system to a stable state is called chaotic control. At present, the main method of controlling fractional-order chaotic systems is to extend the control method used in integer-order chaotic systems to fractional-order chaotic systems. The main methods of chaos control include: parameter perturbation method [33], feedback control method [34], adaptive control method [35], and neural network method [36]. In this section, the chaos control of the fractional-order centrifugal flywheel governor system is realized by using the adaptive control method. The adaptive chaos control formula is derived, and the numerical simulation of chaos control effect is shown.

4.1. Adaptive Chaos Control Scheme. Consider the controlled chaotic system as follows:

$$\begin{cases} D_{t_0}^q x = y + u_1, \\ D_{t_0}^q y = dz^2 \cos x + \left(e + pz^2\right)\sin x \cos x - \sin x - by + u_2, \\ D_{t_0}^q z = s\cos x - F - \alpha \sin(w) + u_3, \\ D_{t_0}^q w = \sigma + u_4, \end{cases} \tag{14}$$

where x, y, z, and w are state variables and u_1, u_2, u_3, and u_4 are external active control inputs. Then, the adaptive control system can be defined by

$$\begin{cases} u_1 = -y - k_1 x, \\ u_2 = -dz^2 \cos x - \left(e + pz^2\right)\sin x \cos x + \sin x + by - k_2 y, \\ u_3 = -\hat{s}(t)\cos x + F + \alpha \sin(w) - k_3 z, \\ u_4 = -\sigma - k_4 w, \end{cases} \tag{15}$$

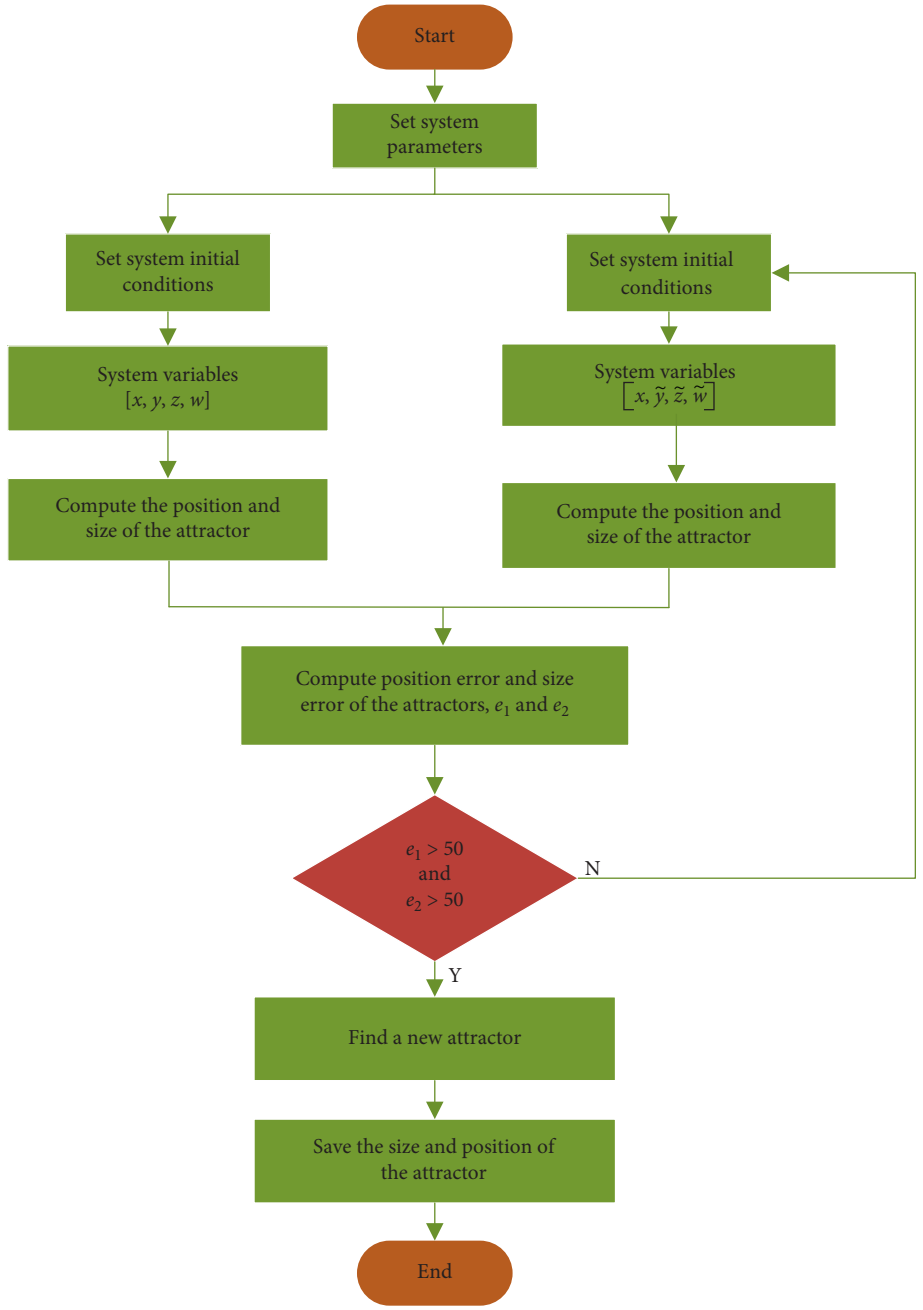

Figure 7: The flow chart for basins of attraction.

where k_1, k_2, k_3, and k_4 are positive gain constants. Substituting (13) into (12), the closed-loop system is obtained as

$$\begin{cases} D_{t_0}^q x = -k_1 x, \\ D_{t_0}^q y = -k_2 y, \\ D_{t_0}^q z = (s - \hat{s}(t))\cos x - k_3 z, \\ D_{t_0}^q w = -k_4 w. \end{cases} \tag{16}$$

Define the parameter s estimation errors as

$$e_s(t) = s - \hat{s}(t). \tag{17}$$

Using (15), we can simplify (14) as

$$\begin{cases} D_{t_0}^q x = -k_1 x, \\ D_{t_0}^q y = -k_2 y, \\ D_{t_0}^q z = e_s(t)\cos x - k_3 z, \\ D_{t_0}^q w = -k_4 w. \end{cases} \tag{18}$$

Differentiating (15) with respect to t, we obtain

$$D_{t_0}^q e_s(t) = -D_{t_0}^q \hat{s}(t). \tag{19}$$

The Lyapunov function is defined by

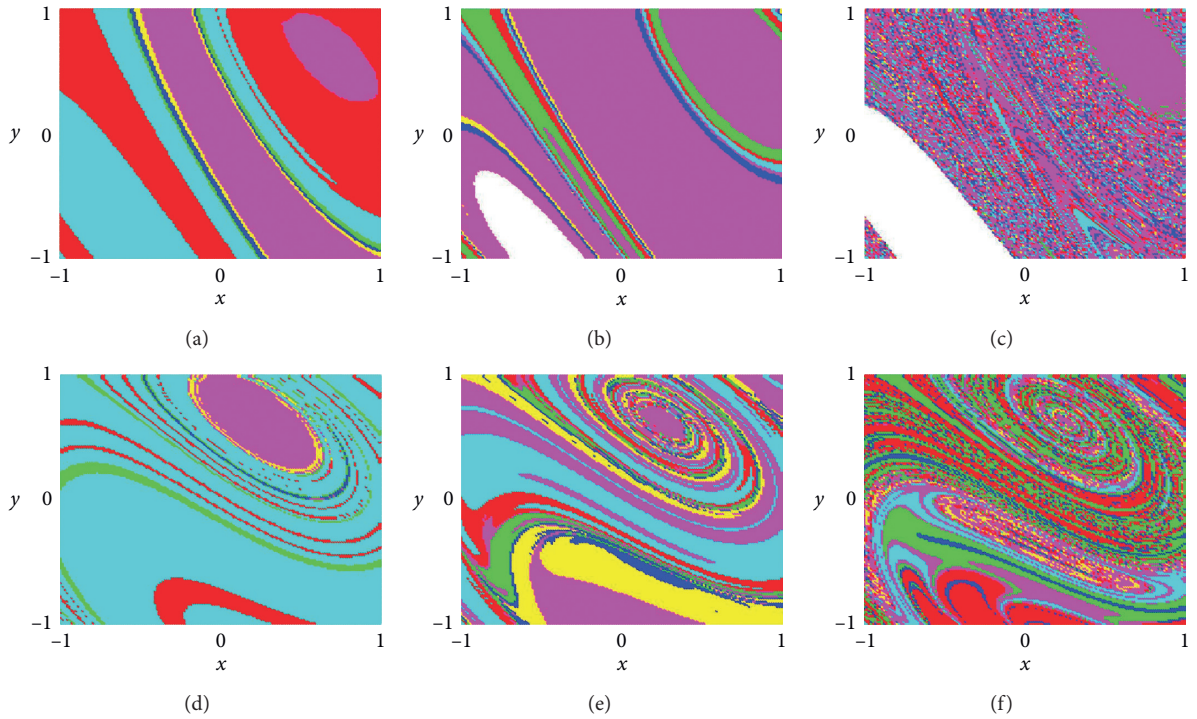

Figure 8: The basins of attraction in the x_0-y_0 plane with different parameters: (a) $s = 10$ and $q = 0.97$; (b) $s = 10$ and $q = 0.98$; (c) $s = 10$ and $q = 0.99$; (d) $s = 5$ and $q = 0.97$; (e) $s = 5$ and $q = 0.98$; (f) $s = 5$ and $q = 0.99$.

$$V(x, y, z, w, e_s) = \frac{1}{2}\left(x^2 + y^2 + z^2 + w^2 + \frac{1}{a}e_s^2\right), \tag{20}$$

where a is a positive convergence factor, the controlling convergence rate of parameter estimation error. Differentiating V, we obtain

$$\begin{aligned} V(x, y, z, w, e_s) = &-k_1x^2 - k_2y^2 - k_3z^2 - k_4w^2 \\ &+ e_s\left(z\cos x - \frac{1}{a}D_{t_0}^q\hat{s}\right). \end{aligned} \tag{21}$$

In view of equation (19), we take the parameter update law as

$$D_{t_0}^q\hat{s} = az\cos x. \tag{22}$$

From the formula derivation process above, it can be seen that the controlled chaotic system (12) is globally and exponentially stabilized by the adaptive control law (13) and the parameter update law (20). By substituting the parameter update law (20) into (19), we obtain the time-derivative of V as

$$V(x, y, z, w, e_s) = -k_1x^2 - k_2y^2 - k_3z^2 - k_4w^2. \tag{23}$$

Equation (21) demonstrates that the Lyapunov function V is positive definite on R^8. According to Barbalat's lemma [37], the closed-loop system (19) is globally exponentially stable for all initial conditions $[x_0, y_0, z_0, w_0] \in R^4$. This completes the proof.

4.2. Numerical Analysis. Fix $q = 0.99$, $s = 10$, in order to better demonstrate the effect of chaos control, the initial conditions are set to a large values as $[x_0, y_0, z_0, w_0] = [1, -2, 2, 4]$, and then phase portraits of the fractional-order centrifugal flywheel governor system are shown in Figure 10. We can see that the system is chaotic under these conditions. Let $k_1 = k_2 = k_3 = k_4 = 10$, the convergence factor $a = 20$, the initial value of parameter s is $s_0 = 4$, and the chaos control results of the system are shown in Figure 11. It can be seen that the chaos control of the fractional-order centrifugal flywheel governor system is successfully realized by the adaptive control method. In 1.5 s, each state component of the system is controlled to the stable state, and the estimation error of parameter s approximates the target value.

In order to further analyze the relationship between the convergence factor a and the estimation error e_s, the estimated error curves of the parameter s with different convergence factor a are obtained in Figure 12. It shows that with the increase in the convergence factor a, the estimation error e_s of parameter s converges faster and faster. When a is greater than or equal to 50, the system approaches the target value within 1 s.

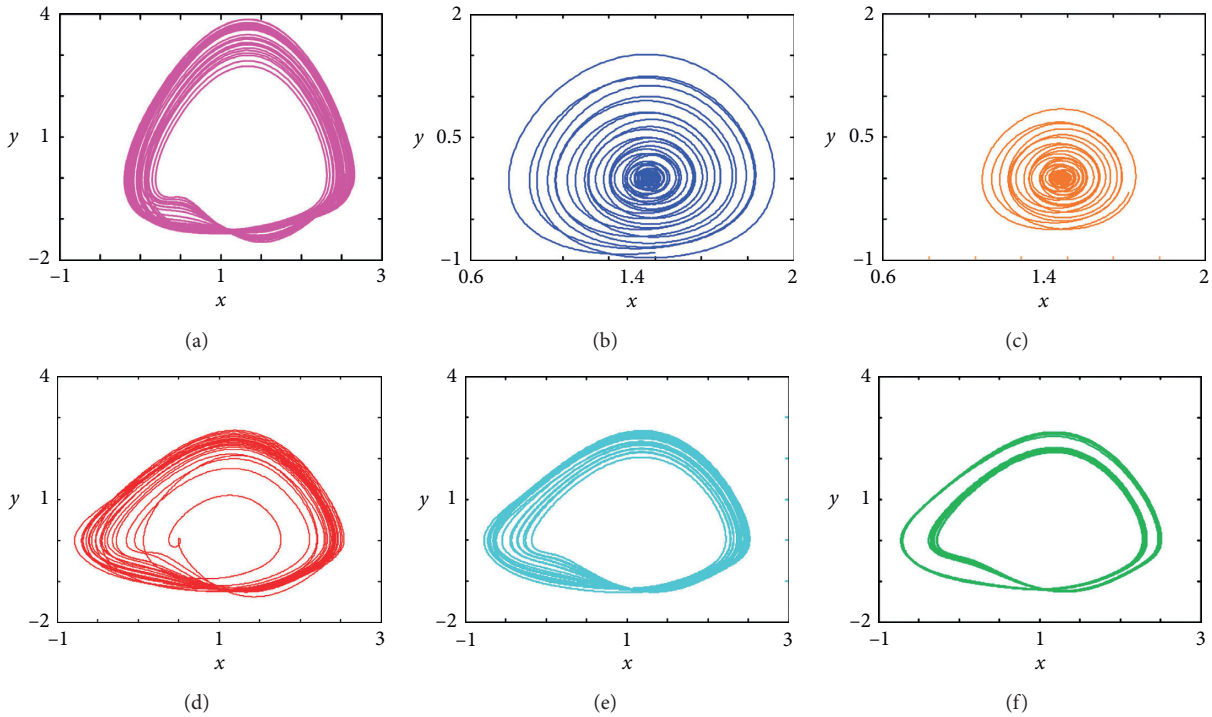

Figure 9: Coexisting attractors with different conditions: (a), (b), (c) $q = 0.98$, $s = 10$, and the initial conditions are [0.005, 0.005, −0.1, 0.1], [0.5, 0.005, −0.1, 0.1], and [0.58, 0.005, −0.1, 0.1]; (d), (e), (f) $q = 0.99$, $s = 5$, and the initial conditions are [−0.9, 0.1, −0.1, 0.1], [−0.9, 0.2, −0.1, 0.1], and [−0.9, 0.82, −0.1, 0.1].

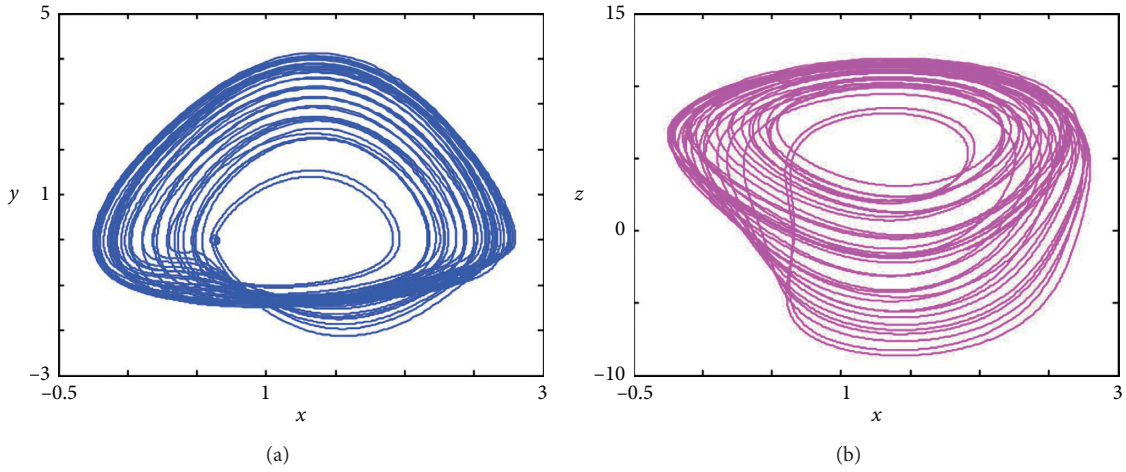

Figure 10: Phase diagrams of the fractional-order centrifugal flywheel governor system with initial values [1, −2, 2, 4].

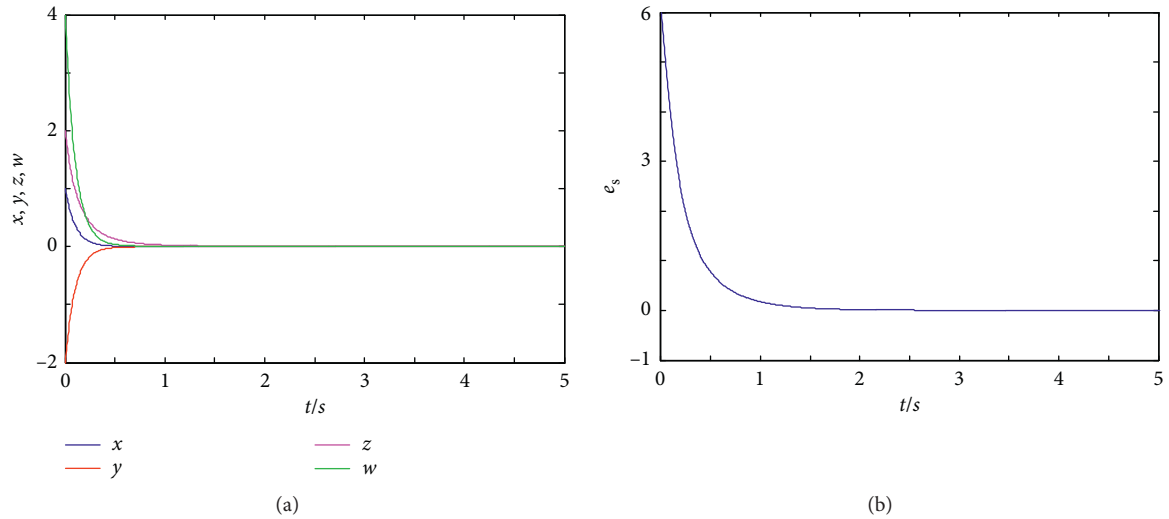

(a) (b)

Figure 11: Control charts of the controlled chaotic system. (a) Time response of state variables. (b) The estimation error of parameter s.

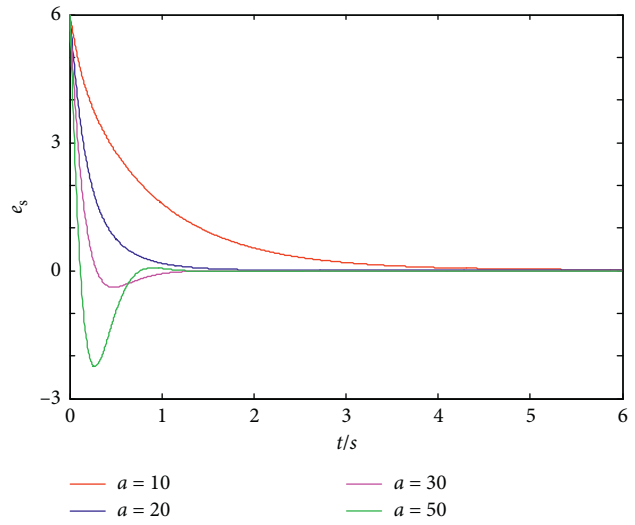

Figure 12: The estimation error of parameter s with different convergence factors.

5. Conclusions

In this paper, dynamics and adaptive control of the fractional-order centrifugal flywheel governor system are investigated. By numerical simulation, the bifurcation diagrams and LEs of the system with different parameters are obtained. The dynamic behavior of the system shown by these two kinds of graphs is in a good agreement, and the LE curve can well describe the process of transition from period to chaos. Coexisting attractors of the system are observed by drawing the basin of attraction, and the attractors with different initial conditions verify the simulation results of the basin of attraction. The adaptive control algorithm designed in this paper effectively realizes the chaos control of the system, and the estimation error e_s of parameter s converges faster and faster with the increase in the convergence factor a.

Data Availability

The data used to support the findings of this study are included within the article.

Conflicts of Interest

The authors declare that they have no conflicts of interest regarding the publication of this paper.

Acknowledgments

This work was supported by the Hunan Provincial Department of Education General Project Fund (no. 18C0743), the National Natural Science Foundation for theoretical physics of China (nos. 61901530 and 11747150), and the Natural Science Foundation of Hunan Province (no. 2020JJ5767).

References

[1] E. J. Beltrami, *Mathematics for Dynamic Modeling*, Academic Press, Cambridge, USA, 1987.

[2] C. Cao, J. Su, and L. Xu, "Chaotic motion of the centrifugal governor," *Journal of Harbin Engineering University*, vol. 18, no. 5, pp. 96–103, 1997.

[3] J. Zhang, Y. Chu, X. Li, and Y. Chang, "Bifurcation and chaos of a type of the centrifugal governor system," *Journal of Mechanical Strength*, vol. 30, no. 3, pp. 362–367, 2008.

[4] X. Gou and G. Luo, "Linear feedback anti-control of chaos for mechanical centrifugal governor system," *Journal of Machine Design*, vol. 22, no. 4, pp. 30–32, 2005.

[5] X. Gou and G. Luo, "Un-feedback chaos controlling problems for mechanical centrifugal governor system," *Journal of Mechanical Strength*, vol. 27, pp. 21–27, 2005.

[6] X. Gou and G. Luo, "Nonlinear feedback anti-control of chaos for mechanical centrifugal flywheel governor systems," *China Mechanical Engineering*, vol. 16, no. 15, pp. 1373–1376, 2005.

[7] J. Wang, H. Wang, and H. Liang, "Chaos and nonlinear feedback control in a flywheel system with a centrifugal

governor," *Mechanical Science and Technology Aerospace Engineering*, vol. 28, no. 2, pp. 238–245, 2009.

[8] J. Wang, H. Wang, and H. Liang, "Chaos and ITS speed feedback control in centrifugal flywheel governor," *Journal of Mechanical Strength*, vol. 32, no. 3, pp. 509–512, 2010.

[9] J. Wang, H. Wang, and H. Liang, "Chaos and control of centrifugal flywheel governor system," *Journal of Machine Design*, vol. 26, no. 9, pp. 34–37, 2009.

[10] J.-G. Zhang, X.-F. Li, Y.-D. Chu, J.-N. Yu, and Y.-X. Chang, "Hopf bifurcations, Lyapunov exponents and control of chaos for a class of centrifugal flywheel governor system Bifurcation and chaos of a type of the centrifugal governor system," *Chaos, Solitons & Fractals*, vol. 39, no. 5, pp. 2150–2168, 2009.

[11] X.-B. Rao, Y.-D. Chu, X. Lu-Xu, Y.-X. Chang, and J.-G. Zhang, "Fractal structures in centrifugal flywheel governor system," *Communications in Nonlinear Science and Numerical Simulation*, vol. 50, pp. 330–339, 2017.

[12] S. Luo, Z. Hou, and T. Zhang, "Performance enhanced design of chaos controller for the mechanical centrifugal flywheel governor system via adaptive dynamic surface control," *AIP Advances*, vol. 6, no. 9, 2016.

[13] M. P. Aghababa and H. P. Aghababa, "Chaos suppression of rotational machine systems via finite-time control method," *Nonlinear Dynamics*, vol. 69, no. 4, pp. 1881–1888, 2012.

[14] R. Zhang, Y. Wang, Z. Zhang, and Q. Bi, "Nonlinear behaviors as well as the bifurcation mechanism in switched dynamical systems," *Nonlinear Dynamics*, vol. 79, no. 1, pp. 465–471, 2015.

[15] R. Gorenflo and F. Mainardi, "Fractional calculus," *Fractals and Fractional Calculus in Continuum Mechanics*, vol. 378, pp. 223–276, 1997.

[16] R. Bhattacharyya, M. Banerjee, M. Heiblum et al., "Melting of interference in the fractional quantum Hall effect: appearance of neutral modes," *Physical Review Letters*, vol. 122, no. 24, Article ID 246801, 2019.

[17] A. C. Escamilla, J. E. Lavín-Delgado, J. F. Gómez-Aguilar, and L. Torres, "Fractional dynamics and synchronization of Kuramoto oscillators with nonlocal, nonsingular and strong memory," *Alexandria Engineering Journal*, vol. 59, no. 4, pp. 1941–1952, 2020.

[18] A. Jajarmi, E. M. Hajipour, and D. Baleanu, "A new approach for the nonlinear fractional optimal control problems with external persistent disturbances," *Journal of the Franklin Institute*, vol. 355, no. 9, pp. 3938–3967, 2018.

[19] P. J. Torvik and R. L. Bagley, "On the appearance of the fractional derivative in the behavior of real materials," *Journal of Applied Mechanics*, vol. 51, no. 2, pp. 725–728, 1984.

[20] Z.-M. Ge and W.-R. Jhuang, "Chaos, control and synchronization of a fractional order rotational mechanical system with a centrifugal governor," *Chaos, Solitons & Fractals*, vol. 33, no. 1, pp. 270–289, 2007.

[21] S. He, K. Sun, and H. Wang, "Solution and dynamics analysis of a fractional-order hyperchaotic system," *Mathematical Methods in the Applied Sciences*, vol. 39, no. 11, pp. 2965–2973, 2016.

[22] Y. Wang, K. Sun, S. He, and H. Wang, "Dynamics of fractional-order sinusoidally forced simplified Lorenz system and its synchronization," *The European Physical Journal Special Topics*, vol. 223, no. 8, pp. 1591–1600, 2014.

[23] D. Kai, N. J. Ford, and A. D. Freed, "A predictor-corrector approach for the numerical solution of fractional differential equations," *Nonlinear Dynamics*, vol. 29, no. 4, pp. 3–22, 2002.

[24] M. F. Oskouie, R. Ansari, and F. Sadeghi, "Nonlinear vibration analysis of fractional viscoelastic Euler-Bernoulli nanobeams based on the surface stress theory," *Acta Mechanica Solida Sinica*, vol. 30, no. 4, pp. 416–424, 2017.

[25] S. He, S. Banerjee, and K. Sun, "Complex dynamics and multiple coexisting attractors in a fractional-order microscopic chemical system," *The European Physical Journal Special Topics*, vol. 228, no. 1, pp. 195–207, 2019.

[26] http://www.sourcecodeonline.com/details/predictorcorrector_pece_method_for_fractional_differential_equations.html.

[27] M.-F. Danca and N. Kuznetsov, "Matlab code for Lyapunov exponents of fractional-order systems," *International Journal of Bifurcation and Chaos*, vol. 28, no. 5, Article ID 1850067, 2018.

[28] B. Yan, S. He, and S. Wang, "Multistability and formation of spiral waves in a fractional-order memristor-based hyperchaotic lu system with No equilibrium points," *Mathematical Problems in Engineering*, vol. 2020, Article ID 2468134, 12 pages, 2020.

[29] Q. Lai, Z. Wan, and P. D. Kamdem Kuate, "Modelling and circuit realisation of a new no-equilibrium chaotic system with hidden attractor and coexisting attractors," *Electronics Letters*, vol. 56, no. 20, p. 1044, 2020.

[30] Q. Lai, Z. Wan, P. D. Kamdem Kuate, and H. Fotsin, "Coexisting attractors, circuit implementation and synchronization control of a new chaotic system evolved from the simplest memristor chaotic circuit," *Communications in Nonlinear Science and Numerical Simulation*, vol. 89, Article ID 105341, 2020.

[31] Q. Lai, B. Norouzi, and F. Liu, "Dynamic analysis, circuit realization, control design and image encryption application of an extended Lü system with coexisting attractors," *Chaos, Solitons & Fractals*, vol. 114, pp. 230–245, 2018.

[32] C. Li and J. C. Sprott, "Multistability in a butterfly flow," *International Journal of Bifurcation and Chaos*, vol. 23, no. 12, Article ID 1350199, 2013.

[33] L. Chen, Y. Chai, and R. Wu, "Linear matrix inequality criteria for robust synchronization of uncertain fractional-order chaotic systems," *Chaos*, vol. 21, no. 4, pp. 251–968, 2011.

[34] J. Chen, C. Li, T. Huang, and X. Yang, "Global stabilization of memristor-based fractional-order neural networks with delay via output-feedback control," *Modern Physics Letters B*, vol. 31, no. 5, p. 1750031, 2017.

[35] C. Lien, S. Vaidyanathan, A. Sambas et al., "A new two-scroll chaotic attractor with three quadratic nonlinearities, its adaptive control and circuit design," *IOP Conference Series: Materials Science and Engineering*, vol. 332, Article ID 012010, 2018.

[36] S. Shao, C. Mou, and J. Wu, "Tracking control for uncertain fractional-order chaotic systems based on disturbance observer and neural network," *Ima Journal of Mathematical Control & Information*, vol. 34, no. 3, pp. 1011–1030, 2017.

[37] F. Wang and Y. Yang, "Correction: fractional order barbalat's lemma and its applications in the stability of fractional order nonlinear systems," *Mathematical Modelling and Analysis*, vol. 22, no. 4, pp. 503–513, 2017.